



Cite this: *Chem. Commun.*, 2020, 56, 8830

Received 5th April 2020,  
Accepted 26th June 2020

DOI: 10.1039/d0cc02463e

rsc.li/chemcomm

## Mixing A $\beta$ (1–40) and A $\beta$ (1–42) peptides generates unique amyloid fibrils†

Linda Cerofolini,<sup>a</sup> Enrico Ravera,<sup>ab</sup> Sara Bologna,<sup>ab</sup> Thomas Wiglenda,<sup>c</sup> Annett Böddrich,<sup>c</sup> Bettina Purfürst,<sup>d</sup> Iryna Benilova,<sup>e</sup> Magdalena Korsak,<sup>f</sup> Gianluca Gallo,<sup>ab</sup> Domenico Rizzo,<sup>ab</sup> Leonardo Gonnelli,<sup>ab</sup> Marco Fragai,<sup>ab</sup> Bart De Strooper,<sup>g</sup> Erich E. Wanker<sup>\*,eg</sup> and Claudio Luchinat<sup>id</sup> <sup>\*,abf</sup>

**Recent structural studies show distinct morphologies for the fibrils of A $\beta$ (1–42) and A $\beta$ (1–40), which are believed not to co-fibrillize. We describe here a novel, structurally-uniform 1 : 1 mixed fibrillar species, which differs from both pure fibrils. It forms preferentially even when A $\beta$ (1–42) : A $\beta$ (1–40) peptides are mixed in a non-stoichiometric ratio.**

Among the major unknowns in Alzheimer's disease research are the mechanisms by which different A $\beta$ (1–42) and/or A $\beta$ (1–40) aggregate species cause toxicity in mammalian cells. Most biophysical studies on A $\beta$  peptides reported in the literature only deal with the behavior of a single alloform of the peptide, and do not consider the many A $\beta$  peptides that coexist *in vivo*.<sup>1–6</sup> However, it has been widely demonstrated that increasing amounts of A $\beta$ (1–42) relative to A $\beta$ (1–40) speed up the aggregation kinetics and also alter the pattern of spontaneously formed oligomeric species,<sup>7–11</sup> which are considered the main toxic

species.<sup>12–14</sup> The rate of formation of these species is markedly different between the two main isoforms.<sup>15,16</sup>

Kuperstein *et al.* have previously reported that all mixtures of A $\beta$ (1–42) and A $\beta$ (1–40) peptides with ratios higher than 3 : 7 are equally prone to aggregation, and show a similar lag-phase.<sup>10</sup> Based on this observation, it was concluded that toxicity results from an increase of the A $\beta$ (1–42)/A $\beta$ (1–40) ratio,<sup>10</sup> suggesting that the properties of mixture do not match the sum of the properties of the two individual components, therefore implying the formation of mixed species. The formation of mixed intermediate species has been proposed,<sup>17</sup> and can be considered the result of the diverse conversion and aggregation pathways of these peptides.<sup>15,18,19</sup> However, it is widely believed that A $\beta$ (1–42) and A $\beta$ (1–40) do not co-fibrillize.<sup>17</sup> Whether the two alloforms interplay or act separately instead is an important question, as this has implications for the propagation of fibrillar seeds in the brain.<sup>20,21</sup>

We have prepared fibrils in the same experimental conditions as those previously used to obtain well-shaped fibrils of pure A $\beta$ (1–40),<sup>22</sup> using a 1 : 1 ratio of the two isoforms (Fig. S1 and S2, ESI†). A new single species is spontaneously formed. The mixtures before fibrillization show a marked toxicity to cultured neurons (see for the characterization Fig. S3, ESI†). When a 3 : 7 A $\beta$ (1–42) : A $\beta$ (1–40) ratio (previously found to be the most toxic mixture<sup>10</sup>) is used, the same single species is observed, but with the excess A $\beta$ (1–40) simultaneously forming the same pure fibrillar species previously characterized by Bertini *et al.*<sup>22</sup> (Fig. S4, ESI†). No cross-peaks among the two species are observable. The ratio between the two species has been estimated from the intensity of the signals in the 2D <sup>13</sup>C–<sup>13</sup>C correlation spectra and found to be approximately 4 : 3, in line with the expectation (see ESI†).

We have acquired solid-state NMR spectra on two samples of the species obtained at the 1 : 1 ratio with either one of the peptides uniformly <sup>13</sup>C–<sup>15</sup>N labeled. The spectra of the labeled A $\beta$ (1–42) and the A $\beta$ (1–40) components in the two 1 : 1 mixed samples are superimposable (Fig. 1). The spectra of the A $\beta$ (1–42)

<sup>a</sup> Magnetic Resonance Center (CERM), University of Florence and Interuniversity Consortium for Magnetic Resonance of Metalloproteins (CIRMMP), Via L. Sacconi 6, 50019, Sesto Fiorentino (FI), Italy. E-mail: claudioluchinat@cerm.unifi.it

<sup>b</sup> Department of Chemistry "Ugo Schiff", University of Florence, Via della Lastruccia 3, 50019, Sesto Fiorentino (FI), Italy

<sup>c</sup> Neuroproteomics, Max Delbrück Center for Molecular Medicine, Robert-Roessle-Strasse 10, 13125 Berlin, Germany. E-mail: ewanker@mdc-berlin.de

<sup>d</sup> Core Facility Electron Microscopy, Max-Delbrück Center for Molecular Medicine, Robert-Roessle-Strasse 10, 13125 Berlin, Germany

<sup>e</sup> VIB Center for Brain and Disease Research, Herestraat 49, 3000 Leuven, Belgium

<sup>f</sup> Giotto Biotech S.R.L., Via Madonna del Piano 6, 50019 Sesto Fiorentino (FI), Italy

<sup>g</sup> KU Leuven, Department of Neurology, Herestraat 49, 3000 Leuven, Belgium.

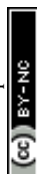
E-mail: bart.destrooper@kuleuven.vib.be

† Electronic supplementary information (ESI) available. See DOI: 10.1039/d0cc02463e

‡ Current address: MRC Prion Unit at UCL, Institute of Prion diseases, Courtauld building, 33 Cleveland Street, London W1W7FF, UK.

§ Current address: Roche Polska Sp. z o. o. Domaniewska 28, 02-672 Warszawa, Poland.

¶ Current address: Fresenius Kabi, Via Camagri 41, Verona, Italy.



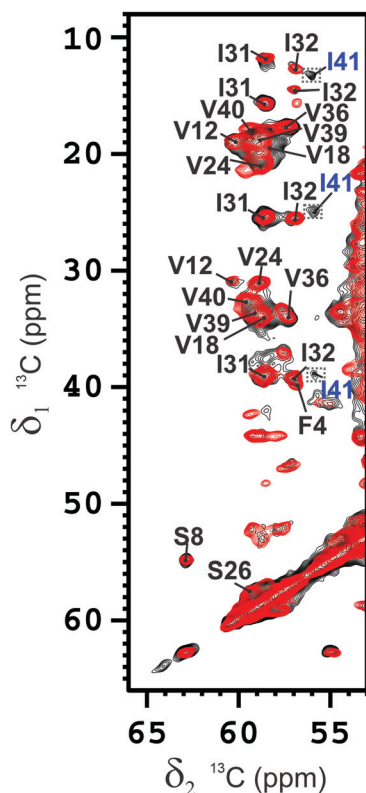
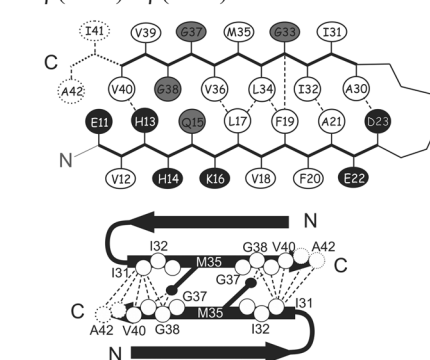


**Fig. 1** Section of the overlaid 2D  $^{13}\text{C}$ – $^{13}\text{C}$ -correlation spectra of the  $\text{A}\beta(1-42)$  component (black) and of the  $\text{A}\beta(1-40)$  component (red) in the 1 : 1  $\text{A}\beta(1-42)$  :  $\text{A}\beta(1-40)$  mixed fibrils. Mixing time = 100 ms. Magnetic field: 700 MHz (16.4 T), dimension of rotor: 3.2 mm (~14 mg of fibrils), 12 kHz spinning, 100 kHz  $^1\text{H}$  decoupling,  $T = 283$  K. The resonances are assigned as indicated. The crosspeaks corresponding to I41 are magnified by a factor 2.

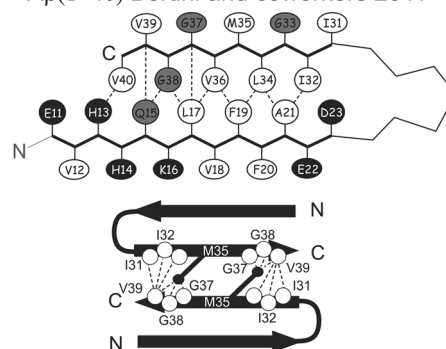
component show some extra peaks (particularly for S8 and G9), suggesting that the  $\text{A}\beta(1-42)$  may be more rigid than the  $\text{A}\beta(1-40)$  in the N-terminal loop, as well as a few minor peaks attributable to other species, possibly linked to a slight imbalance in the concentration of the two isoforms. When assigned<sup>23,24</sup> (Fig. S6 and S7, ESI<sup>†</sup>), the spectra yield the same intra- and intermolecular contacts, showing that the conformation of the two peptides is identical. Signals correlating the side chains of Leu17 with Leu34/Val36, Phe19 with Gly33/Leu34, Ala21 with Ile32, and His13 with Val40 were detected and assigned unambiguously on the  $^{13}\text{C}$ – $^{13}\text{C}$  correlation<sup>25</sup> spectra at different mixing times on both samples (see Table S1, ESI<sup>†</sup>). These contacts are only consistent with a U-shaped conformation of the monomer typical of  $\text{A}\beta(1-40)$  and not with the characteristic S-shaped conformation of  $\text{A}\beta(1-42)$  (Scheme S1, ESI<sup>†</sup>).

When the unambiguous contacts are reported on the topology of the monomer, it is clear that in the  $\beta$ -arch the reciprocal packing of the two  $\beta$ -strands ( $\beta_1$  and  $\beta_2$ ) (Fig. S8A, ESI<sup>†</sup>), is different from that of pure  $\text{A}\beta(1-40)$  obtained in the same conditions<sup>22</sup> (Fig. S8B, ESI<sup>†</sup> and Scheme 1) and, instead, resembles that reported for fibrils of pure  $\text{A}\beta(1-40)$  or  $\text{A}\beta(1-42)$  obtained under different conditions by Tycko and Smith and coworkers<sup>2,26,27</sup> (Scheme S1, see ESI<sup>†</sup> for the details of structure

### $\text{A}\beta(1-40)$ : $\text{A}\beta(1-42)$ mixed fibrils



### $\text{A}\beta(1-40)$ Bertini and coworkers 2011



**Scheme 1** Topologies of monomer and the interprotofilament interface identified in the present work and in previously studied pure  $\text{A}\beta(1-40)$ .<sup>22</sup> The dashed/dotted lines represent unambiguous experimental restraints used to derive the corresponding topology. In the schematic description of the monomer, the hydrophobic, acidic/basic, and other types of residues are shown in white, black, and gray, respectively. The filled black circles represent the  $\text{C}_\epsilon$  of the Met35 residue. Other residues included in SS-NMR-observed structural restraints for linking the protofilaments are shown as hollow circles.

calculations), and has also the same register of the highly toxic oligomers stabilized by an intramolecular disulfide bond between residues 21 and 30, mutated to cysteine.<sup>28</sup>

As previously observed,<sup>22</sup> Lys28 is exposed to the solvent and not involved in the formation of salt-bridges.<sup>29–32</sup> The analysis of the cross-peaks in the  $^{13}\text{C}$ – $^{13}\text{C}$  correlation spectra supports the presence of a parallel arrangement of the protein molecules along the  $\beta$ -spine. No cross-peaks correlating the N-terminus and C-terminus of  $\beta_1$  or  $\beta_2$  strands have been observed in the spectrum of either sample. This indicates that the  $\beta$ -strand-turn- $\beta$ -strand motif is organized in parallel cross- $\beta$  sheets as reported in the literature for mature fibrils of  $\text{A}\beta(1-40)$ .<sup>2,22,26,27,33,34</sup> This model is further supported by the presence of a single pattern of signals for each residue in the SS-NMR spectra. For symmetry considerations, this is consistent only with the presence of a parallel in-register  $\beta$ -spine.<sup>35</sup> Each of the  $\beta$ -spines constituting the sides of the cross- $\beta$  sheet arrangement is called “protofilament” for simplicity.

More specifically, the  $\beta_1$ – $\beta_2$  arrangement of the 1–40 filaments of both  $\text{A}\beta(1-40)$  and  $\text{A}\beta(1-42)$  are identical in the mixed fibrils.



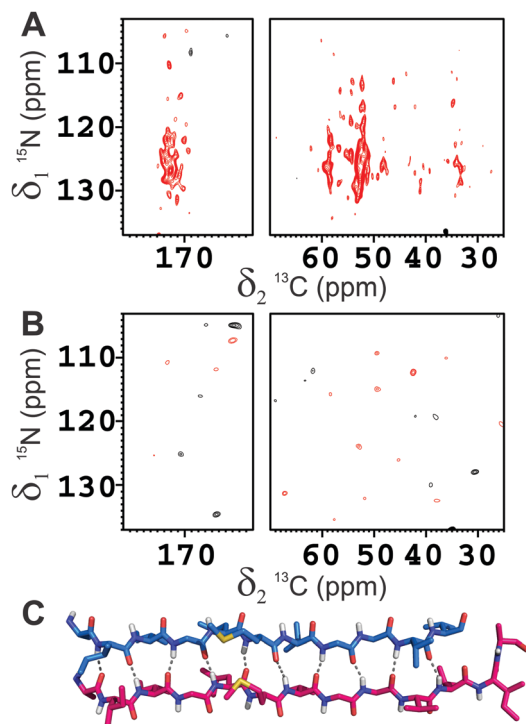


**Fig. 2** 2D  $^{15}\text{N}$ - $^{13}\text{C}$  hNhhC spectra of the A $\beta$ (1-42):A $\beta$ (1-40) mixed fibrils in the 1:1 molar ratio, where (A) A $\beta$ (1-42) is  $^{15}\text{N}$ -enriched and A $\beta$ (1-40) is  $^{13}\text{C}$ -enriched, (B) A $\beta$ (1-42) is  $^{15}\text{N}$ -enriched and A $\beta$ (1-40) is in natural abundance. Magnetic field: 800 MHz (19 T, 201.2 MHz  $^{13}\text{C}$  Larmor frequency), dimension of rotor: 3.2 mm, 16 kHz spinning, 80 kHz  $^1\text{H}$  decoupling; number of scans: 2048. The strong cross peaks in the carbonyl and  $\text{C}_\alpha$  regions in (A) and the total absence of signals in (B) clearly demonstrates that the transfer in (A) is occurring between the two alloforms. (C) The H-bonds pattern of A $\beta$ (1-42) interlaced with A $\beta$ (1-40) in the  $\beta$ -spine is displayed.

Homogeneous protofilaments of either A $\beta$ (1-40) or A $\beta$ (1-42) can be excluded by the presence in the spectra of cross-peaks between N-terminus and C-terminus of the  $\beta_2$  strand, which would not be present if all the labeled peptide molecules were in the same protofibril (Fig. S9 and S10, ESI $^\dagger$ ). We are thus left with the possibility of an interlaced arrangement. To further prove this, fibrils from 1:1 mixtures of  $^{15}\text{N}$ -enriched A $\beta$ (1-42) and  $^{13}\text{C}$ -enriched A $\beta$ (1-40) were prepared, in such a way as to have NMR signals only if  $^{15}\text{N}$  and  $^{13}\text{C}$  nuclei are in close proximity. In particular, a two-dimensional nitrogen-carbon correlation experiment, 2D  $^{15}\text{N}$ - $^{13}\text{C}$  hNhhC<sup>36</sup> shows good signal intensity in several parts of the spectrum and particularly in the NH-carbonyl region, thus demonstrating direct, short range contacts between A $\beta$ (1-40) and A $\beta$ (1-42) filaments (Fig. 2), further confirmed by a 1D TEDOR experiment (Fig. S11, ESI $^\dagger$ ).<sup>37</sup> These data demonstrate beyond any doubt that A $\beta$ (1-40) and A $\beta$ (1-42) can co-fibrillize in a 1:1 ratio to form an interlaced fibril (Fig. 3 and Fig. S12, ESI $^\dagger$ ).

The heterogeneity observed in the SS-NMR spectra of pure A $\beta$ (1-42) under the present conditions may reflect the endpoint of a fast aggregation reaction, which is instead prevented by the formation of a 1:1 product when A $\beta$ (1-40) and A $\beta$ (1-42) are present simultaneously in solution and which also favors a

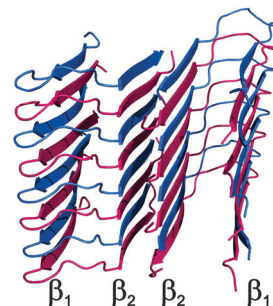
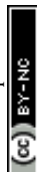


**Fig. 3** Structural model of A $\beta$ (1-40)/A $\beta$ (1-42) interlaced mixed fibrils. The A $\beta$ (1-42) polypeptide is colored in magenta while the A $\beta$ (1-40) polypeptide in blue.

conformation with the turn at positions G25 and S26 over the one with the turn at positions E22 and D23, which are putatively involved in the toxicity of early aggregates.<sup>38,39</sup> In the present interlaced fibrils, the observed U-shape register ideally accommodates the requirements of both filaments, and is likely to provide an extra stabilization by preventing the steric clashes potentially caused by Ile41 and Ala42 because these two residues are alternatively present and absent in the interlaced fibrils. The buried surface area is maximum for the mixture in this arrangement, see Table S5 (ESI $^\dagger$ ).

The present observation that a single fibrillary species is obtained from mixtures of A $\beta$ (1-42) and A $\beta$ (1-40) indicates that the interplay between the two alloforms may contribute to extend the number of possible polymorphs formed by these peptides, increasing the complexity of the structural landscape of the amyloid aggregates, which may correspond to phenotypic differences.<sup>40</sup> We expect that the availability of a structural model for this mixed-species will be useful for a better understanding of the variable nature of cross-seeding,<sup>29,41,42</sup> as well as in the development of potential drugs.<sup>43,44</sup>

This research activity has been supported by EC funding initiative ERA-NET NEURON ABETA ID ("Novel Methods and Approaches towards the Understanding of Brain Diseases"), funded by the German Federal Ministry for Education and Research (BMBF), grant no. 01W1301, by the Fonds voor Wetenschappelijk Onderzoek (FWO) and the Italian Ministero della Salute. BDS is supported by the FWO, the KU Leuven and VIB, a Methusalem grant of the KU Leuven/Flemish Government and by the Bax-Vanluffelen Chair for Alzheimer's Disease and "Opening the Future" of the Leuven Universiteit Fonds. Support has been provided also by: Fondazione CRFirenze, MIUR ("Progetto Dipartimenti di Eccellenza 2018-2022" and PRIN 2017A2KEPL), the Helmholtz Validation Fund grant no. HVF-0013 "Enabling Technologies for Drug Discovery against Protein Misfolding Diseases" by the Helmholtz Association, Germany and the Berlin Institute of Health Collaborative Research Grant no. 1.1.2.a.3 "Elucidating the proteostasis network to control Alzheimer's disease", funded by the BMBF. The Italy CERM/CIRMMP centre of INSTRUCT-ERIC is also acknowledged. This work was also supported by Instruct-ULTRA (Grant 731005), an EU H2020 project to further develop the services of Instruct-ERIC.



## Conflicts of interest

There are no conflicts to declare.

## Notes and references

|| Structures formed by a molar excess of A $\beta$ (1–42) were not analyzed, but A $\beta$ (1–42) by itself yields a strongly heterogeneous mixture under the present conditions (Fig. S5, ESI†).

- 1 R. Tycko, *Protein Sci.*, 2014, **23**, 1528–1539.
- 2 A. K. Paravastu, R. D. Leapman, W.-M. Yau and R. Tycko, *Proc. Natl. Acad. Sci. U. S. A.*, 2008, **105**, 18349–18354.
- 3 Y. Qi-Takahara, M. Morishima-Kawashima, Y. Tanimura, G. Dolios, N. Hirotsu, Y. Horikoshi, F. Kametani, M. Maeda, T. C. Saido, R. Wang and Y. Ihara, *J. Neurosci.*, 2005, **25**, 436–445.
- 4 D. M. Bolduc, D. R. Montagna, M. C. Seghers, M. S. Wolfe and D. J. Selkoe, *eLife*, 2016, **5**, e17578.
- 5 J.-P. Colletier, A. Laganowsky, M. Landau, M. Zhao, A. B. Soriaga, L. Goldschmidt, D. Flot, D. Cascio, M. R. Sawaya and D. Eisenberg, *Proc. Natl. Acad. Sci. U. S. A.*, 2011, **108**, 16938–16943.
- 6 D. M. Bolduc and M. S. Wolfe, *Proc. Natl. Acad. Sci. U. S. A.*, 2014, **111**, 14643–14644.
- 7 Y. Yoshiike, D.-H. Chui, T. Akagi, N. Tanaka and A. Takashima, *J. Biol. Chem.*, 2003, **278**, 23648–23655.
- 8 A. Jan, O. Gokce, R. Luthi-Carter and H. A. Lashuel, *J. Biol. Chem.*, 2008, **283**, 28176–28189.
- 9 A. Jan, D. M. Hartley and H. A. Lashuel, *Nat. Protocols*, 2010, **5**, 1186–1209.
- 10 I. Kuperstein, K. Broersen, I. Benilova, J. Rozenski, W. Jonckheere, M. Debulpaep, A. Vandersteen, I. Segers-Nolten, K. Van Der Werf, V. Subramaniam, D. Braeken, G. Callewaert, C. Bartic, R. D'Hooge, I. C. Martins, F. Rousseau, J. Schymkowitz and B. De Strooper, *EMBO J.*, 2010, **29**, 3408–3420.
- 11 K. Pauwels, T. L. Williams, K. L. Morris, W. Jonckheere, A. Vandersteen, G. Kelly, J. Schymkowitz, F. Rousseau, A. Pastore, L. C. Serpell and K. Broersen, *J. Biol. Chem.*, 2012, **287**, 5650–5660.
- 12 B. R. Sahoo, S. J. Cox and A. Ramamoorthy, *Chem. Commun.*, 2020, **56**, 4627–4639.
- 13 D. M. Walsh, I. Klyubin, J. V. Fadeeva, W. K. Cullen, R. Anwyl, M. S. Wolfe, M. J. Rowan and D. J. Selkoe, *Nature*, 2002, **416**, 535–539.
- 14 K. Ono, *Neurochem. Int.*, 2018, **119**, 57–70.
- 15 G. Bellomo, S. Bologna, L. Gonnelli, E. Ravera, M. Fragai, M. Lelli and C. Luchinat, *Chem. Commun.*, 2018, **54**, 7601–7604.
- 16 T. C. T. Michaels, A. Šarić, S. Curk, K. Bernfur, P. Arosio, G. Meisl, A. J. Dear, S. I. A. Cohen, C. M. Dobson, M. Vendruscolo, S. Linse and T. P. J. Knowles, *Nat. Chem.*, 2020, **12**, 445–451.
- 17 R. Cukalevski, X. Yang, G. Meisl, U. Weininger, K. Bernfur, B. Frohm, T. P. J. Knowles and S. Linse, *Chem. Sci.*, 2015, **6**, 4215–4233.
- 18 Y. Lin, B. R. Sahoo, D. Ozawa, M. Kinoshita, J. Kang, M. H. Lim, M. Okumura, Y. H. Huh, E. Moon, J. H. Jang, H.-J. Lee, K.-Y. Ryu, S. Ham, H.-S. Won, K.-S. Ryu, T. Sugiki, J. K. Bang, H.-S. Hoe, T. Fujiwara, A. Ramamoorthy and Y.-H. Lee, *ACS Nano*, 2019, **13**, 8766–8783.
- 19 I. Bertini, G. Gallo, M. Korsak, C. Luchinat, J. Mao and E. Ravera, *ChemBioChem*, 2013, **14**, 1891–1897.
- 20 R. Tycko, *Nature*, 2016, **537**, 492–493.
- 21 M. Jucker and L. C. Walker, *Nat. Neurosci.*, 2018, **21**, 1341–1349.
- 22 I. Bertini, L. Gonnelli, C. Luchinat, J. Mao and A. Nesi, *J. Am. Chem. Soc.*, 2011, **133**, 16013–16022.
- 23 A. Schuetz, C. Wasmer, B. Habenstein, R. Verel, J. Greenwald, R. Riek, A. Böckmann and B. H. Meier, *ChemBioChem*, 2010, **11**, 1543–1551.
- 24 S. Sun, Y. Han, S. Paramasivam, S. Yan, A. E. Siglin, J. C. Williams, I.-J. L. Byeon, J. Ahn, A. M. Gronenborn and T. Polenova, in *Protein NMR Techniques*, ed. A. Shekhtman and D. S. Burz, Humana Press, Totowa, NJ, 2012, pp. 303–331.
- 25 B. Hu, O. Lafon, J. Trébosc, Q. Chen and J.-P. Amoureux, *J. Magn. Reson.*, 2011, **212**, 320–329.
- 26 A. T. Petkova, W.-M. Yau and R. Tycko, *Biochemistry*, 2006, **45**, 498–512.
- 27 M. Ahmed, J. Davis, D. Aucoin, T. Sato, S. Ahuja, S. Aimoto, J. I. Elliott, W. E. Van Nostrand and S. O. Smith, *Nat. Struct. Mol. Biol.*, 2010, **17**, 561–567.
- 28 A. Sandberg, L. M. Luheshi, S. Söllvander, T. P. de Barros, B. Macao, T. P. J. Knowles, H. Biverstål, C. Lendel, F. Ekholm-Pettersson, A. Dubnovitsky, L. Lannfelt, C. M. Dobson and T. Härd, *Proc. Natl. Acad. Sci. U. S. A.*, 2010, **107**, 15595–15600.
- 29 Y. Xiao, B. Ma, D. McElheny, S. Parthasarathy, F. Long, M. Hoshi, R. Nussinov and Y. Ishii, *Nat. Struct. Mol. Biol.*, 2015, **22**, 499–505.
- 30 M. T. Colvin, R. Silvers, Q. Z. Ni, T. V. Can, I. Sergeyev, M. Rosay, K. J. Donovan, B. Michael, J. Wall, S. Linse and R. G. Griffin, *J. Am. Chem. Soc.*, 2016, **138**, 9663–9674.
- 31 J.-X. Lu, W. Qiang, W.-M. Yau, C. D. Schwieters, S. C. Meredith and R. Tycko, *Cell*, 2013, **154**, 1257–1268.
- 32 A. T. Petkova, R. D. Leapman, Z. Guo, W.-M. Yau, M. P. Mattson and R. Tycko, *Science*, 2005, **307**, 262–265.
- 33 A. T. Petkova, Y. Ishii, J. J. Balbach, O. N. Antzutkin, R. D. Leapman, F. Delaglio and R. Tycko, *Proc. Natl. Acad. Sci. U. S. A.*, 2002, **99**, 16742–16747.
- 34 W. Qiang, W.-M. Yau, Y. Luo, M. P. Mattson and R. Tycko, *Proc. Natl. Acad. Sci. U. S. A.*, 2012, **109**, 4443–4448.
- 35 J. T. Nielsen, M. Bjerring, M. D. Jeppesen, R. O. Pedersen, J. M. Pedersen, K. L. Hein, T. Vosegaard, T. Skrydstrup, D. E. Otzen and N. C. Nielsen, *Angew. Chem., Int. Ed.*, 2009, **48**, 2118–2121.
- 36 A. Lange, S. Becker, K. Seidel, K. Giller, O. Pongs and M. Baldus, *Angew. Chem., Int. Ed.*, 2005, **44**, 2089–2092.
- 37 C. P. Jaronec, C. Filip and R. G. Griffin, *J. Am. Chem. Soc.*, 2002, **124**, 10728–10742.
- 38 Y. Matsushima, R. C. Yanagita and K. Irie, *Chem. Commun.*, 2020, **56**, 4118–4121.
- 39 A. R. Foley, H.-W. Lee and J. A. Raskatov, *J. Org. Chem.*, 2020, **85**, 1385–1391.
- 40 J. Stöhr, C. Condello, J. C. Watts, L. Bloch, A. Oehler, M. Nick, S. J. DeArmond, K. Giles, W. F. DeGrado and S. B. Prusiner, *Proc. Natl. Acad. Sci. U. S. A.*, 2014, **111**, 10329–10334.
- 41 M. Törnquist, R. Cukalevski, U. Weininger, G. Meisl, T. P. J. Knowles, T. Leiding, A. Malmendal, M. Akke and S. Linse, *Proc. Natl. Acad. Sci. U. S. A.*, 2020, **117**(21), 11265–11273.
- 42 J. Tran, D. Chang, F. Hsu, H. Wang and Z. Guo, *FEBS Lett.*, 2017, **591**, 177–185.
- 43 M. Zhang, J. Zheng, R. Nussinov and B. Ma, *Antibodies*, 2018, **7**(3), 25.
- 44 J. Zhao, R. Nussinov and B. Ma, *J. Biol. Chem.*, 2017, **292**, 18325–18343.

